3808 J. Agric. Food Chem. 2009, 57, 3808–3817
DOI:10.1021/jf8033144

JOURNAL OF AGRICULTURAL AND FOOD CHEMISTRY
ARTICLE

Differentially-Expressed Genes in Pig *Longissimus* Muscles with Contrasting Levels of Fat, as Identified by Combined Transcriptomic, Reverse Transcription PCR, and Proteomic Analyses

Jingshun Liu,[†] Marie Damon,[†] Nathalie Guitton,[‡] Isabelle Guisle,[§] Patrick Ecolan,[†] Annie Vincent,[†] Pierre Cherel,[∥] and Florence Gondret*,[†]

[†]INRA, UMR1079 Systèmes d'Elevage Nutrition Animale et Humaine, 35590 Saint Gilles, France, [‡]High-Throughput Proteomics Platform OUEST-Genopole, 263 Avenue du Général Leclerc, Bâtiment 24, Campus de Beaulieu, 35042 Rennes, France, [§]INSERM U533, Faculté de Médecine, 44035 Nantes, France and [∥]France Hybrides, 100, Avenue Denis Papin, 45808 Saint Jean de Braye Cedex, France

Intramuscular fat content is important for many meat quality parameters. This work is aimed at identifying functional categories of genes associated with natural variation among individuals in intramuscular fat content to help the design of genetic schemes for high marbling potential. Taking advantage of the global nature of transcriptomic and proteomic technologies, 40 genes were identified as differently expressed between high fat and low fat pig *Longissimus* muscles at slaughter weight. They are involved in metabolic processes, cell communication, binding, and response to stimulus. Using real-time PCR in muscle biopsies taken earlier in the fattening period, the group with a high intramuscular fat content was also characterized by the down-expression of genes playing a negative role in adipogenesis, such as architectural transcription factor high-motility hook A1, mitogen activated protein-kinase14, and cyclin D1. These results suggest that interindividual variability in intramuscular fat content might arise essentially from differences in early adipogenesis.

KEYWORDS: Gene expression; intramuscular fat; *Longissimus* muscle; microarray; pig; proteome analysis

INTRODUCTION

Intramuscular (i.m.) fat is an important component of meat quality (see ref *1* for a review). The acceptability of pork may be improved by increasing the i.m. fat level (*2*). Many efforts have been made during the past decades to identify key factors (see ref *3* for a review) and genes involved in the regulation of i. m. fat content. Many studies point out indicators of de novo fatty acid synthesis (*4*, *5*), intracellular fatty acid binding proteins (*6*, *7*), or oxidative metabolism (*8*), to be associated with variations in i.m. fat content in various species. However, the biological mechanisms responsible for variability in this trait are not completely understood until now. Importantly, i.m. fat stores are found both inside the myocytes (*9*) and in adipocytes clustered along the myofiber fasciculi (*10*). The global nature of genomics technology could be an advantage for elucidating the complex physiological control of i.m. fat content, which is likely mediated through multiple biochemical and molecular mechanisms in both adipocytes and myofibers. Microarrays have been recently used in beef muscles to examine gene expressions at different developmental stages and between two breeds with a different propensity to accumulate i.m. fat (*11*, *12*). However, it cannot be excluded that the differences seen in gene expressions are due to breed characteristics rather than to variations in i.m. fat per se. Proteomics has the advantage over cDNA microarrays in that it measures the functional product (protein) of gene expression. Until now, it has, however, been rarely used to address directly the question of i.m. fat variation in domestic animals ((*13*) in trout).

The current study aimed to improve our understanding on the mechanisms and key genes underlying interindividual variability in i.m. fat content, by associating microarray profiling and two-dimensional electrophoresis (2-DE)-based comparative protein patterns in pig *Longissimus* muscles (LM) chosen as extremes for this trait. Because i.m. fat is the latest fat deposit to develop (*14*), genomics investigations were performed on pork meat obtained at commercial slaughter age. In addition, biopsies taken one month before were considered to investigate the earlier expression of target genes.

MATERIALS AND METHODS

Animals and Muscle Sampling. Animals originated from a population of 1,000 pigs generated as an F2 intercross between two production sire lines: FH016 (Pietrain type, France Hybrides SA, St. Jean de Braye, France) and FH019 (Synthetic line from Duroc, Hampshire and Large White founders, France Hybrides SA, St. Jean de Braye, France). All piglets were weaned at 28 days of age and then were fed standard commercial diets during growth. Procedures and slaughtering facilities were

*Corresponding author. Tel: +33 2 23 48 57 52. Fax: +33 2 23 48 50 80. E-mail: Florence.gondret@rennes.inra.fr.

 Published on Web 3/18/2009

approved by the French Veterinary Services. At 70 kg live weight, biopsies were taken in LM at the last rib level. The same time point has been chosen to predict the content in i.m. fat at commercial slaughter weight in a recent pig selection experiment (*7*). The biopsy lasted <1 s, and muscle samples (approximately 100 mg) were immediately frozen and stored at -70 °C. At 110 kg body weight, all pigs were killed according to standard procedures in a commercial slaughterhouse (ORLEANS Viandes, Fleury-les-Aubrais, France). The hot carcass was weighed. Backfat and muscle thickness were measured in predefined locations at the third/fourth lumbar vertebra and third/fourth last rib levels on the carcass, using a hand-held optical probe Fat-O-Meter (SFK, Herlev, Denmark). On the basis of the measurements, a formula was also used to predict lean meat percentage (*15*). A 5 g sample of LM was collected on all pigs 20 min after stunning at the last rib position, immediately frozen in liquid nitrogen, and stored at -70 °C before RNA and protein extractions. The half-carcasses were chilled at 12 °C for a 4 h postmortem, and then stored at 3 °C. The next day, meat pH was recorded in situ in LM at the last rib level, before the carcass was cut. The entire LM was then harvested and weighed. At 36 h postmortem, loins were sliced at the last rib level. One slice was used for chemical analyses (fat content and glycolytic potential). The second slice was used for color measurements.

Intramuscular Fat Content. Total lipids were extracted in duplicate from freeze-dried LM using a 17-fold dilution of tissue in 2:1 chloroform/methanol (vol/vol) according to the method outlined by Folch (*16*). Lipid content of fresh tissue (g/100 g) was obtained by taking into account the dry matter content determined from the weight of minced LM tissues before and after freeze-drying.

Glycolytic Potential. One gram of LM was homogenized into 10 mL of 0.55 M perchloric acid. Glycolytic potential (GP) was then calculated according to Monin and Sellier (*17*), as GP = 2([glycogen] + [glucose] + [glucose-6-phosphate]) + [lactate]. Metabolites were determined by reference methods based on the enzymatic reaction with hexokinase (for glucose) or on enzymatic colorimetric reaction under the influence of lactate oxidase (for lactate). Commercially available kits (glucose HK, ABX Diagnostics kit, Montpellier, France and lactate PAP, Biomerieux, Marcy l'Etoile, France) were used on an automatic spectrophotometric analyzer (Cobas Mira Roche, Basel, Switzerland). Muscle glycogen content was determined from glucose determination after hydrolysis by amiloglucosidase. GP was expressed as μmol lactate equivalent/g of wet tissue.

pH. One gram of LM sample collected 20 min after slaughter was incubated at 39 °C for 25 min and then dispersed (Ultra turrax, Ika-Werke GmbH, Staufen, Germany) in 9 mL of 5 mM sodium-iodoacetate buffer (pH 7.0). The pH (pH1) was then measured on this solution within 4 h after dispersion, using a glass/KCl electrode (N1041A, Schott AG, Mainz, Germany) and a Knick 766 benchtop pH meter (Knick Elektronische Messgerate GmbH & Co., Berlin, Germany). Meat ultimate pH (pHu) was recorded 24 h postmortem in situ in LM using an Ingold Xerolyt penetration gel electrode (Mettler Toledo SA, Viroflay, France) and a portable Knick 911 pH meter (Knick Elektronische Messgerate GmbH & Co., Berlin, Germany).

Color. Color was recorded on three 10 mm diameter spots from each LM eye rib surface within 2 h following loin slicing. Indicators of lightness (L*), redness (a*), and yellowness (b*) were recorded using a Minolta CR300 colorimeter (Konica Minolta Sensing Europe BV, Roissy, France), and the average value of the three spots was used.

Microarray Experiment. From the 1,000 pigs slaughtered at 110 kg body weight, two groups of 8 each were then chosen from the extremes as illustrated in **Figure 1** to have either a low (1.36 ± 0.21%, [LF], $n = 6$ females and $n = 2$ barrows) or a high (4.58 ± 0.30%, [HF], $n = 3$ females and $n = 5$ barrows) lipid content at this stage. Transcriptome analysis was performed on these LM samples using 50-mer oligonucleotide microarrays designed from 5726 human and 955 murine genes expressed in normal and pathological skeletal and cardiac muscles (MyoChip, OuestGenopole, Nantes, France, http://cardioserve.nantes.inserm.fr/ptf-puce/spip.php?article18). These muscle-specific genes encoded proteins implicated in 13 biological processes according to gene ontology (GO) annotations. Each gene was spotted in triplicate with 3141 control spots (buffer and empty), allowing statistical studies of the reproducibility of the hybridization experiments to be performed.

Total RNA was extracted from LM samples as described previously (*18*) and purified using RNeasy MinElute Kit (Qiagen, Hilden, Germany). RNA concentration was evaluated by ND-1000 Spectrophotometer (NanoDrop Technologies, Wilmington, DE), and RNA quality was assessed using an Agilent Bioanalyser 2100 (Agilent Technologies, Santa-Clara,

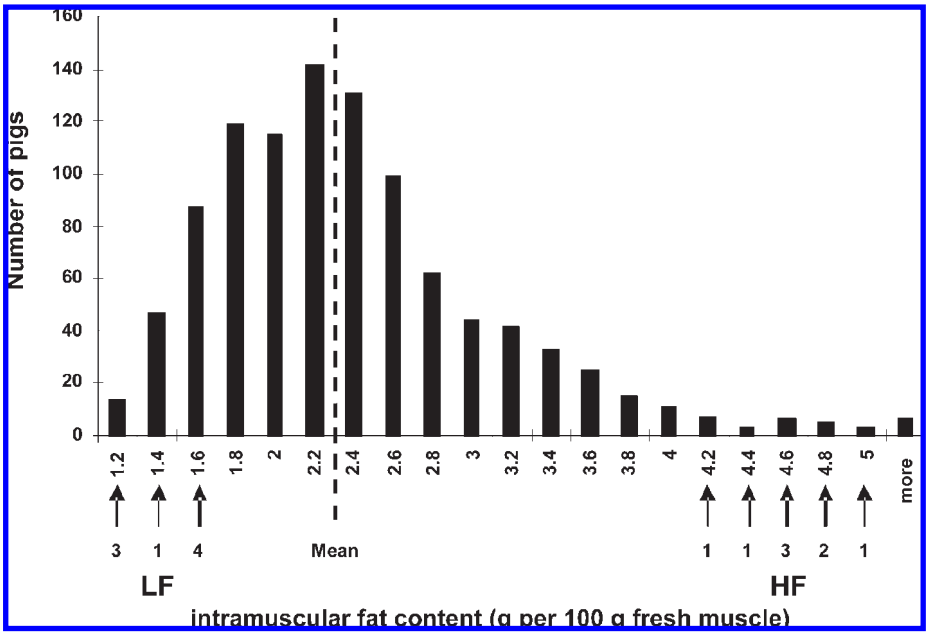

Figure 1. Distribution of intramuscular fat content in *Longissimus* muscle of pigs at 110 kg body weight. Black arrows indicate the number of pigs chosen for having either high (4.58 ± 0.30%, $n = 8$, [HF]) or low (1.36 ± 0.21%, $n = 8$, [LF]) intramuscular fat content. The broken line stands for the mean of intramuscular fat content in the population.

CA). To compare animal groups in the microarray experiments, each sample has to be compared to a reference pool composed of an equal amount of transcripts isolated from one group (*19*). In the current experiment, the reference pool was composed of the 8 LF samples. Total RNA (500 ng) from each animal was labeled individually with Cy3 by using the Amino Allyl MessageAmp II aRNA Amplification kit (Applied Biosystems, Courtaboeuf, France), following the manufacturer's instructions. Samples were then mixed with an equal amount of the reference pool labeled with Cy5. Each sample was hybridized in duplicate at the Transcriptome Core Facility of OuestGenopole (Nantes, France). The slides were preincubated in a solution containing 3.5× SSC, 0.3% SDS, and 1% BSA at 42 °C for 60 min to prevent nonspecific hybridization. Probes were then resuspended in 40 μL of hybridization buffer (*19*), containing poly (A) RNA (0.5 μg/μL) and Yeast RNA (0.5 μg/μL), Denhardt (5×), 3.5× SSC, 0.3% SDS, and 50% formamide denatured at 98 °C, and then hybridized overnight at 42 °C. The slides were then washed sequentially for 2 min each in 2× SSC with 0.1% SDS, 1× SSC, and 0.2× SSC, and then spin-dried.

Protein Extraction and Electrophoresis. Muscle samples (approximately 100 mg each) of a subset of the same LF (n = 4 females and 2 barrows) and HF (n = 3 females and 3 barrows) pigs at 110-kg slaughter weight, were ground thoroughly to a very fine powder under liquid nitrogen using a mortar and pestle. They were then homogenized in 1 mL of a 0.25 M sucrose buffer (pH 7.4) at 4 °C containing 1 mM dithiolthreitol, 1 mM EDTA, and complete protease inhibitors (Roche, Mannheim, Germany) using a glass bead agitator (Heidolph, Schwabach, Germany). The homogenates were then centrifuged at 100,000*g* at 4 °C for 1 h, and the supernatants (below the fat cake) representing cytosolic proteins were collected. Cytosolic fractions were then precipitated by adding 1 volume of 10% trichloroacetic acid solution. The resulting protein pellets were washed in acetone solution (v/v) three times. After centrifugation at 12,000*g* during 5 min, the pellets were quickly dried at room temperature. They were dissolved in 250 μL of lysis buffer containing 7.5 M urea (GE Healthcare, Orsay, France), 2 M thiourea (Sigma, Saint-Quentin Fallavier, France), 2% CHAPS (GE Healthcare), 40 mM Tris (Sigma), 2.5 μL of IPG buffer 3−10 NL (GE Healthcare), and cocktail protease inhibitors (Sigma) by incubating at room temperature for 1 h with small magnetic rails. The total protein concentration was assessed by the Bradford assay (BioRad, Hercules, CA). The homogenates were then stored at −70 °C until used later for electrophoresis.

Cytosolic proteins (80 μg for analytical gel, 200 to 600 μg for preparative gel) were then loaded by the addition of Destreack solution (GE Healthcare) and 2% carrier ampholytes, to make up the volume to 450 μL. Precast immobilized gradient (IPG) gel strips (24 cm, 3−10 pH nonlinear, GE Healthcare) were rehydrated in a passive way with the cytosolic proteins over a period of 16 h. Proteins were then isoelectrically focused on an Ettan IPGphorII system (GE Healthcare). A voltage of 150 V was applied initially, followed by a stepwise increase to 8000 V, and reaching a total of 88590 Vh. Subsequently, the IPG strips were equilibrated by soaking for 12 min each at room temperature in a solution containing 50 mM Tris-HCL at pH 8.8, 6 M urea, 2% SDS (v/w), 30% glycerol (v/v), and bromophenol blue as a dye, containing 65 mM DTT (first incubation), or 4.5% iodoacetamide (second incubation). Strips were then applied to the top of a 12.5% SDS−PAGE gel and run in a vertical system (Ettan DALTsix, GE Healthcare). Gels were run at 5 W per gel for 45 min, plus 17 W per gel until the dye reached the bottom of the gels. Analytical gels were made in duplicate per sample and were then visualized by sensitive silver staining (*20*). Then, two master gels were made as preparative gels on equal amounts of the 12 protein extracts and stained according to Shevchenko and colleagues (*21*) to allow further mass spectrometry analysis.

Data Analyses and Statistics. Hybridized microarrays were scanned at 10 μm/pixel resolution on a ScanArray Express 4000 XL (PerkinElmer, Waltham, MA). Image analyses were performed with Genepix Pro 5.0 (Axon Instruments, Union City, CA). Intensities of selected spots were transformed into log (Cy3/Cy5), and data were normalized by both spot and chip by the weighted linear regression (LOWESS) method, using the GeneSpring software (Silicon Genetics, Redwood, CA). Expression values were also analyzed using MADSCAN [http://cardioserve.nantes.inserm.fr/mad/madscan/(*22*)] to obtain experimentally consolidated gene expression values. The MADSCAN procedure uses the median intensities after background corrections and the analytical parameters provided by GenePix Pro to perform physical validation and quality filtration based on four criteria (image analysis flags, signal-to-noise level, diameter variation, and saturation level). All together, 1573 genes were retained for statistical analyses. Transcriptomic data were analyzed using the microarray software package GeneSpring GX 7.3 (Silicon Genetics, Santa-Clara, CA) with the fixed effects of the i.m. fat group (G: HF or LF), hybridization reaction (H: 2 per RNA extraction), and their interaction (G × H). Data were then subjected to the multiple testing correction procedure using the false discovery rate [FDR] ≤ 5% (*23*). The results were expressed according to the fold-change value (FC), which represents the expression ratio of the HF group to the LF group. Therefore, a gene was declared to be up-regulated or down-regulated when its expression was greater (FC > 1) or lower (FC < 1), respectively, in HF group than in LF group. The microarray information has been deposited in the National Center for Biotechnology Information Gene Express Omnibus (GEO) Web site (http://www.ncbi.nlm.nih.gov/geo/) and is publicly available through GEO Series accession no. GSE10759.

Silver-stained analytical gels were scanned using UMAX ImageScanner (GE Healthcare) and analyzed by ImageMaster 2D Platinum 6.0 (GE Healthcare). After automated detection and matching of the 24 gels, highly saturated areas or badly defined spots were manually removed. Spots were then normalized by expressing the relative volume of each spot as the ratio of individual spot volume on the total volume of valid spots. This measure takes into account variations due to protein loading and staining by considering the total volume over all the spots in the image. Data were then analyzed by analysis of variance using SAS software (SAS Inst., Inc.; Cary, NC) and the ANOVA procedure (*24*), with the fixed effects of the i.m. fat group (G: HF or LF) and gel replicate (R: 2 per sample), and their interaction (G × R). $P \leq 0.05$ was retained for significance. The results were expressed according to fold-change value (FC), which represents the expression ratio of the HF group to the LF group.

Analysis of variance (GLM procedure of SAS) was finally used with the i.m. fat group as the main effect to test the significance of the differences in carcass composition and meat characteristics. A $P \leq 0.05$ was retained for significance.

Protein Identification by Mass Spectrometry. The protein spots of biological interest ($P \leq 0.05$) were punched out of the preparative gels using pipet tips. Gel pieces were placed into a 1.5 mL microcentrifuge tube in a solution of 1% acetic acid. Excised spots were processed and digested with trypsin as described previously (*25*). Extraction was performed in two successive steps by adding 50% v/v acetonitrile (ACN)/0.1% trifluoric acid (TFA). Digests were dried out and dissolved with 2 mg/mL α-cyano-4-hydroxycinnamic acid in 70% ACN/0.1% TFA, before spotting onto MALDI targets (384 Scout MTP 600 μm AnchorChip, Bruker Daltonik, Bremen, Germany). Mass fingerprints were acquired using a MALDI combined with a TOF/TOF mass spectrometer (Ultraflex, Bruker Daltonik) and processed with the Flex Analysis software (V2.2, Bruker Daltonik) on the high throughput proteomic facilities of OuestGenopole (Rennes, France). Autolysis products of trypsin were used for internal calibration. The monoisotopic masses of tryptic peptides were used to query NCBI nonredundant sequences databases of all mammalian proteins using the MASCOT search engine (http://www.matrixscience.com). Search conditions were

Table 1. Primer Sequences Used in Quantitative Real-Time PCR

gene symbol	accession no.	forward primer (5′)[a]	reverse primer (3′)[a]
CCND1	BP464451	CACGACTTCATCGAGCACTT	GTTTGCGGATGATCTGTTTG
C/EBPα	AY700218	GTGGACAAGAACAGCAACGA	CTCCAGCACCTTCTGTTGAG
ERK1	AK231529	ACCAGCTCAACCACATTCTG	GTAGTTTCGGGCCTTCATGT
ESD	NM_214060	CACGGCCTTGTCGTCATTG	GCCAAAATCCCAGCTCTCATC
FABP4	AJ416020	GGAAAGTCAAGAGCACCATAACCT	ATTCCACCACCAACTTATCATCTACTATTT
HMGA1	BP166125	GAAAAGGACGGCACTGAGA	TTTTAGGTGTTGGCACTTCG
p38MAPK14	BX669435	GCTCCTGAGATCATGCTGAA	ATTATGCATCCCACTGACCA
PPARγ	DQ437885	ATTCCCGAGAGCTGATCCAA	TGGAACCCCGAGGCTTTAT

[a] All primer sequences were designed using PrimerExpress software.

as follows: an initial rather open mass window of 70 ppm for an internal calibration, one missed cleavage allowed, modifications of cysteines by iodoacetamide, and methionine oxidation and N-terminal pyroglutamylation as variable modifications. To avoid incorrect identifications, 4 matched peptides per protein were required at least, and each matching was carefully checked manually by considering the MASCOT probabilistic score and accuracy of the experimental to theoretical pI and molecular weight (MW). The MASCOT baseline significant score is 68% of coverage of the entire amino acid sequence.

Gene Ontology Analysis. Lists of genes showing a significant difference in the mRNA level between groups for low or high i.m. fat content and those encoding proteins with a differential abundance between the same animals were classified according to their biological process description provided in GO Consortium (www.ncbi.nlm.nih.gov/sites/entrez?Db=gene) for *Homo sapiens*. When the biological process term for a given molecule was lacking, the molecular function description was considered.

Real Time RT-PCR. To investigate the early expression of target genes, total RNA was also extracted from muscles biopsied in the same HF and LF pigs at 70 kg live weight (n = 6 per group). Complementary DNA was synthesized from 2 μg of total DNase-treated RNA in 40 μL of reaction buffer using random primers and murine Moloney leukemia virus reverse transcriptase according to the manufacturer's instructions (Applied Biosystems, Foster City, CA). Expression level of the gene encoding esterase D was studied as a validation of proteomic results in RNA samples extracted from 70-kg biopsies and 110 kg LM samples. Expression level of the adipocyte (A)-type fatty acid binding protein (*FABP4*) encoding a protein that is exclusively expressed in adipocytes (see ref *26* for a review) was also monitored in the same tissues. In addition, six genes related to adipogenesis were also analyzed in the RNA samples at the two times. These genes have been shown to promote differentiation and lipid storage [i.e., the master regulators peroxisome proliferator-activated receptor gamma *PPARγ*, and CCAAT-enhancer binding protein alpha *c/EBPα*; see ref *27* for a review], help in the accessibility of genes to transcription factors [the high mobility family group A1, *HMGA1*; see ref *27* for a review], control G1-S transition of the cell cycle [cyclin D1 *CCND1*(*28*)], or play pivotal roles in cellular processes such as the intracellular mitogen activated protein kinases (MAPK) comprising extracellular signal-regulated kinase *ERK1* and *p38MAPK14* (see ref *29* for a review). Primers (**Table 1**) were designed using the Primer Express software (Applied Biosystems) and were based on *Sus Scrofa* sequences. Amplification was performed starting with 5 ng of reverse-transcribed RNA and both sense and antisense primers (200 nM each), in 12.5 μL of PCR buffer (SYBRGreen I PCR core reagents, Applied Biosystems). An ABI PRISM 7000 SDS thermal cycler (Applied Biosystems) was used. Each reaction was performed in triplicate. The thermal cycling condition was as follows: 95 °C for 10 min, followed by 40 cycles of denaturation at 95 °C for 15 s, and annealing at 59 °C for 60 s. Uracil DNA glycosylase 1 U/100 μL (Invitrogen, Cergy Pontoise, France) was applied to prevent any contamination from previous PCR. Specificity of the amplification products was checked by dissociation curves analysis. Endogenous 18S rRNA amplifications were used for each sample to normalize the expression of the selected genes, using a human 18S rRNA predeveloped TaqMan kit (Applied Biosystems, Courtaboeuf, France). Because PCR efficiencies for target genes and 18S were close to 1 (0.99 + 0.03), the amount of the specific target normalized to 18S, and relative to a calibrator (i.e., one sample of the LF group), was calculated according to the following formula (*30*): ratio $= 2^{-\Delta CTtarget\ (sample\ -\ calibrator)} / 2^{-\Delta CT18S(sample\ -\ calibrator)}$. Levels of mRNAs were then compared between HF and LF samples by Student's t-test. A $P \leq 0.05$ was retained for significance.

Table 2. Mean and Standard Deviation of Carcass Data and Meat Traits and Group Effect

item carcass data	LF group N = 8	HF group N = 8	P values[b]
hot carcass weight, kg	92.8 ± 3.4	92.0 ± 2.4	0.842
backfat depth, mm	14.5 ± 1.1	17.5 ± 1.5	0.122
muscle depth, mm	57.2 ± 2.3	57.6 ± 2.5	0.913
lean meat content, %	62.9 ± 0.7	60.5 ± 1.1	0.100
LM weight, kg	11.1 ± 0.6	10.2 ± 0.3	0.195
meat characteristics[a]			
intramuscular lipid content %	1.3 ± 0.1	4.6 ± 0.1	<0.001
pH_1	6.4 ± 0.1	6.4 ± 0.1	0.865
pH_u	5.6 ± 0.1	5.6 ± 0.1	0.471
GP, micromol lactate/g of muscle	165.2 ± 13.8	174.9 ± 10.1	0.581
L*	49.9 ± 0.6	51.6 ± 0.8	0.118
a*	7.6 ± 0.4	8.4 ± 0.4	0.143
b*	4.8 ± 0.4	6.0 ± 0.4	0.039

[a] pHu, ultimate pH; pH1, pH at 20 min; GP, glycolytic potential; L*, lightness; a*, redness; b*, yellowness; LF, *Longissimus* muscle with a low fat content; HF, *Longissimus* muscle with a high fat content. [b] Differences between HF and LF groups are considered to be significant for P values less than 0.05.

RESULTS

Carcass Composition and Meat Characteristics. As shown in **Table 2**, backfat depth and meat characteristics (except i.m. fat content) did not differ between HF and LF pigs, except a greater yellow index (b*) in the former group compared to that of the latter group.

Transcriptomic Analysis. The hybridization results showed that about 85% of the spots pass quality control criteria. Statistic analyses identified 29 genes that were differentially expressed (FDR ≤ 5%) between LF pigs and HF pigs. As shown in **Table 3**, these genes encoded proteins that are involved in eight functional categories: metabolic process, cell communication, response to stimulus, binding, chromatin assembly, transport, regulation of transcription, and cell proliferation. The ontology of two of these genes was unknown. Among the 29 differentially expressed genes, 63% were up-regulated in the HF group compared to that in the LF group. Importantly, the list of differentially expressed genes between HF and LF pigs did not include the

Table 3. Up- or Down-Regulated Genes between High-Fat and Low-Fat Groups in Pig *Longissimus* Muscle at 110 kg Body Weight

symbol	gene name	FC[a]	GO classification[b]	functional category[b]
Up-Regulated				
MRPS21	mitochondrial ribosomal protein S21	**	translation	metabolic process
SDHA	succinate dehydrogenase complex subunit A	*	tricarboxylic acid cycle	metabolic process
DOLPP1	dolichyl pyrophosphate phosphatase 1	**	protein amino acid N-linked glycosylation	metabolic process
GSTP1	glutathione *S*-transferase pi	**	metabolic process	metabolic process
CA14	carbonic anhydrase XIV	*	one-carbon compound metabolic process	metabolic process
ADSL	adenylosuccinate lyase	**	purine ribonucleotide biosynthetic process	metabolic process
GPR18	G protein-coupled receptor 18	**	signal transduction	cell communication
SEMA3B	semaphorin 3B	*	cell-cell signaling	cell communication
EGFR	epidermal growth factor receptor	*	signaling pathway	cell communication
RNF214	ring finger protein 214	*	protein binding	binding
HIST2H2AA4	histone cluster 2 H2aa4	*	chromatin assembly	chromatin assembly
HIST1H2AE	histone cluster 1 H2ae	*	nucleosome assembly	chromatin assembly
TIMP2	inhibitor of matrix metalloproteinase 2	*	negative regulation of cell proliferation	cell proliferation
POLR2L	polymerase (RNA) II (DNA directed) polypeptide L	*	regulation of transcription	regulation of transcription
TANC2	tetratricopeptide repeat, ankyrin repeat and coiled-coil containing 2	*	regulation of transcription	regulation of transcription
TRIM28	tripartite motif protein 28	*	regulation of transcription from RNA polymerase II promoter	regulation of transcription
A2BP1	ataxin 2-binding protein 1	*	RNA transport	transport
FAM129A	family with sequence similarity 129, member A	*	unknown	unknown
TM9SF1	transmembrane 9 superfamily member 1	*	integral to membrane	unknown
Down-Regulated				
RBP3	retinol binding protein 3	**	lipid metabolic process	metabolic process
MMP24	matrix metallopeptidase 24	*	proteolysis	metabolic process
CXCR3	chemokine (C-X-C motif) receptor 3	*	signal transduction	cell communication
INPP4A	inositol polyphosphate-4-phosphatase type I	*	signal transduction	cell communication
SH2D3C	SH2 domain containing 3C	*	JNK cascade	cell communication
CD48	CD48 molecule	*	defense response	response to stimulus
HSF2	heat shock transcription factor 2	*	response to stress	response to stimulus
KRT17	keratin 17	*	structural constituent	binding
BARHL2	barH-like homeobox 2	*	regulation of transcription	regulation of transcription
MCOLN3	mucolipin 3	**	ion transport	transport

[a] The fold change value (FC) represents the expression ratio of HF to LF samples: *, 0.80 < FC < 1.20; **, FC ≥ 1.20 or FC ≤ 0.80. [b] Gene ontology (GO) classification was performed according to biological process terms, and parent functional category was then added.

well-known master regulators of adipogenesis and lipid accumulation, such as PPARγ, C/EBPα, and sterol-regulatory binding protein (*SREBP*)-1.

Proteomic Analysis. About 437 ± 62 spots on average were detected and analyzed on typical 2-DE gels (**Figure 2**). Twenty-one spots were different ($P \leq 0.05$) between the HF group and LF group. About 64% of these spots have been successfully identified using MALDI-TOF mass spectrometry (**Table 4**). Among them, six proteins are involved in various metabolic processes: the proteasome subunit α type 1 (PSMA1) and the proteasome 26S subunit 4 (PSMC4) are related to protein degradation, enolase (ENO1) and glyceraldehyde-3-phosphate (GAPDH) are involved in glycolysis, glutathione *S*-transferase π (GSTP1) catalyzes the conjugation of reduced glutathione to a wide range of electrophiles, and aldehyde dehydrogenase (ALDH7A1) is associated with the detoxification of aldehydes. The first five proteins had a greater abundance in HF pigs than in LF pigs, whereas the last protein showed a lower abundance in the former compared to the latter pigs. Two proteins involved in cell response to stimulus had a greater representation in HF pigs than in LF pigs: the peroxiredoxin 6 (PRDX6) protects against oxidative damage and DJ-1 (PARK7) functions as a redox-sensitive chaperone. A subunit of protein kinase (PKA) contributes to cell communication. Opposite regulation patterns were shown for two binding proteins: calcium-binding parvalbumin (PVALB) and cofilin (CFL2). Finally, esterase D (ESD), with hydrolase activity but without annotation in the GO database, had a lower abundance in HF pigs than in LF pigs. Except ALDH7A1, all of these proteins are encoded by genes that are spotted on the microarrays.

Functional Categories Shared by Transcriptomic and Proteomic Lists. Only *GSTP1* was found differently expressed at both the mRNA and protein levels. The functional distribution of the 40 unique genes with a difference in the mRNA level (*29*) or encoding proteins (*12*) with a differential abundance between HF and LF pigs is shown in **Figure 3**. Four main categories were shared by transcriptomic and proteomic lists: metabolic process accounting for 32.5% of the differentially expressed unique genes, cell communication (17.5%), binding (10%), and response to stimulus (10%). Protein, peptide, and glucose metabolisms were well-represented in the metabolic process pathway (22.5%) both at the mRNA and protein abundance levels (**Figure 3B**). On the contrary, categories encompassing the regulation of transcription, chromatin assembly, transport, and negative regulation of cell proliferation were represented by few genes differentially expressed at the mRNA level only.

Real Time RT-PCR. In muscle biopsies taken in pigs at 70-kg live weight, the mRNA level of ESD was lower in the HF group than in the LF group (**Table 5**). In addition, expression levels of *HMGA1*, *CCND1*, and *p38MAPK14* were lower in biopsies of the HF group compared to the LF group (**Table 5**). On the contrary, the *FABP4* mRNA level was 1.4-fold greater in HF biopsies than in LF ones. Finally, expression levels of the two master regulators of adipogenesis *PPARγ* and *C/EBPα* did not differ ($P > 0.10$) between the two biopsy groups. Expression levels of all of

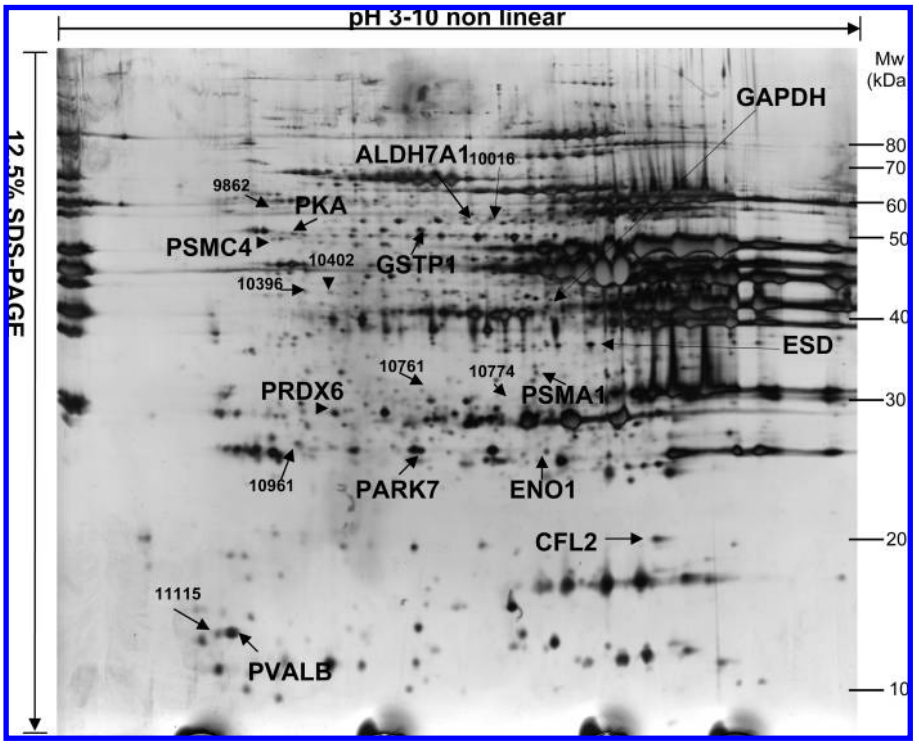

Figure 2. Representative 2-dimensional electrophoretic gel in pig *Longissimus* muscle. Cytosolic proteins were extracted in muscles of pigs at 110 kg body weight. Protein spots that were differentially represented ($P \leq 0.05$) between pig muscles having either high (HF, $n = 6$) or low (LF, $n = 6$) fat content are shown. Abbreviations used: ALDH7A1, aldehyde dehydrogenase 7 family; CFL2, cofilin 2; ENO1, enolase; ESD, esterase D; GAPDH, glyceraldehyde-3-phosphate dehydrogenase GSTP1, glutathione-*S*-transferase pi; PARK7, DJ-1 protein; PKA, RIα subunit of cyclic adenosine 5′-monophosphate (cAMP)-dependent protein kinase; PRDX6, peroxiredoxin 6; PSMA1, proteasome subunit α type 1; PSMC4, proteasome 26S ATPase subunit 4; PVALB, parvalbumin.

Table 4. Proteins Differentially Represented between High-Fat and Low-Fat Groups in Pig *Longissimus* Muscle at 110 kg Body Weight

symbol	protein name	accession number[a]	sequence coverage (%)[b]	theoretical pI/Mw (kDa)[c]	MASCOT score[d]	FC[e]	GO classification[f]	functional category[f]
Proteins Having a Greater Abundance								
PSMA1	proteasome subunit alpha type 1	XP508298	38	7.68/41.1	103	**	ubiquitin-dependent protein catabolic process	metabolic process
PSMC4	proteasome 26S ATPase subunit 4	NP476463	25	5.09/47.5	63	**	proteolysis	metabolic process
GSTP1	glutathione-*S*-transferase	S13780	52	7.30/23.3	86	**	metabolic process	metabolic process
GAPDH	glyceraldehyde-3-phosphate dehydrogenase	NP001029206	41	8.50/36.1	96	**	glycolysis	metabolic process
ENO1	enolase protein	AAH21166	49	5.87/29.2	102	**	Glycolysis	metabolic process
PARK7	DJ-1 protein	NP001072131	80	6.33/20.1	164	**	respond to hydrogen peroxide	response to stimulus
PRDX6	peroxiredoxin 6	NP999573	37	5.73/25.1	91	**	response to oxidative stress	response to stimulus
PVALB	parvalbumin	NP001069582	54	5.16/12.1	84	**	calcium ion binding	binding
Proteins Having a Lower Abundance								
ALDH7A1	aldehyde dehydrogenase 7 family	NP001039434	30	5.69/55.9	81	**	aldehyde metabolic process	metabolic process
PKA	RIα subunit of cyclic adenosine 5′-monophosphate (cAMP)-dependent protein kinase	1NE4A	50	5.04/31.9	140	**	intracellular signaling cascade	cell communication
CFL2	cofilin 2	NP068733	55	7.66/18.8	85	**	Actin binding	binding
ESD	esterase D	NP999225	44	6.54/32.0	116	**	hydrolase activity	unknown

[a] Protein names and accession numbers were derived from the NCBI database. [b] Percent of coverage of the entire aminoacid sequence. [c] Mw and pI were recorded in the NCBI database. [d] The MASCOT baseline significant score is 68. [e] The fold change value (FC) represents the ratio of abundance between HF pigs and LF pigs. **, FC > 1.20 or FC < 0.80. [f] Gene ontology (GO) classification was performed according to biological process terms, except CFL2, PVALB, and ESD for which molecular function descriptions were considered, and parent functional category was then added.

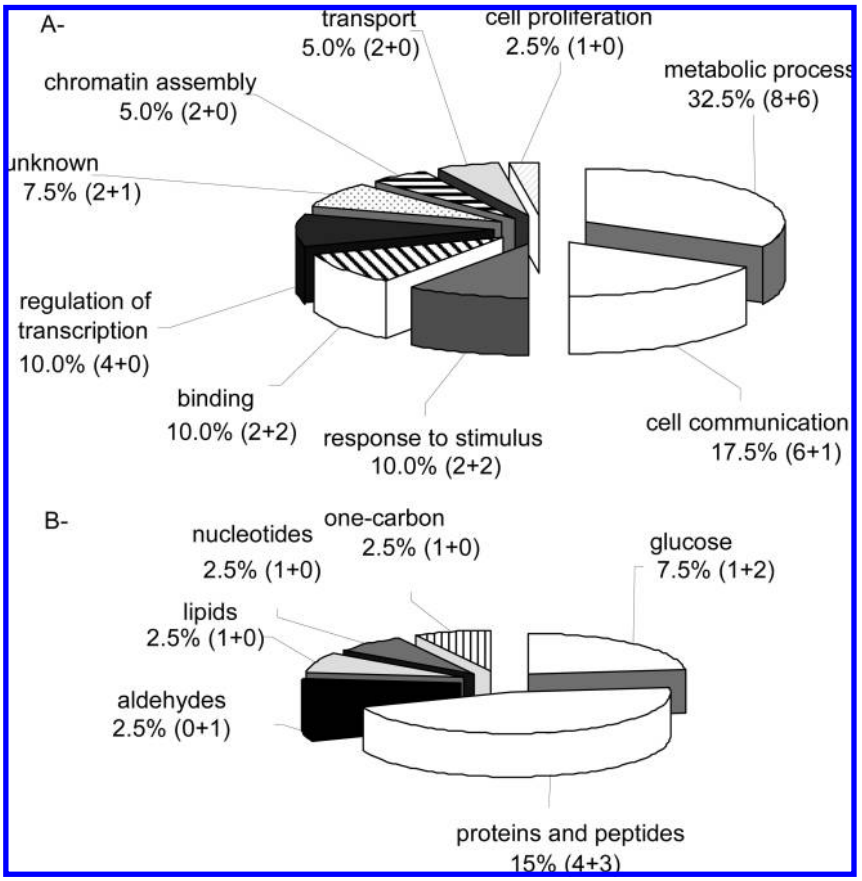

Figure 3. Functional classification of differentially expressed genes and proteins. The numbers of genes with a differential mRNA level or having different protein abundance, respectively, are indicated in each category. Glutathione-*S*-transferase π (*GSTP1*) was found differentially expressed at both the mRNA and protein levels in the metabolic process. Therefore, the relative percentage of each category was calculated from 40 unique genes. (**A**) The chart represents the different categories for the biological process. (**B**) The chart represents the details for metabolic process subcategories.

Table 5. Differential Expression of Candidate Genes by Real Time RT-PCR in High-Fat and Low-Fat Groups in *Longissimus* Muscle Biopsied in Pigs at 70 kg Live Weight

		gene expression[a]		
symbol	gene name	LF group	HF group	*P* values[b]
ESD	esterase D	0.98 ± 0.30	0.60 ± 0.17	0.029
FABP4	adipocyte-type fatty acid binding protein	1.27 ± 0.11	1.73 ± 0.13	0.028
PPARγ	peroxisome proliferator-activated receptor gamma	1.19 ± 0.92	0.57 ± 0.24	0.146
C/EBPα	CCAAT enhancer binding protein alpha	1.31 ± 1.32	0.62 ± 0.34	0.250
CCND1	cyclin D1	0.89 ± 0.37	0.38 ± 0.08	0.009
HMGA1	high mobility group AT-hook 1	1.13 ± 0.31	0.67 ± 0.30	0.035
ERK1	extracellular signal-regulated kinases 1	1.50 ± 1.22	1.22 ± 1.10	0.447
p38MAPK14	mitogen activated protein kinase 14	1.09 ± 0.34	0.75 ± 0.16	0.050

[a] Levels of mRNA (arbitrary units) for selected genes were normalized to the level of 18S rRNA in the same samples. [b] Differences in gene expression levels between HF and LF biopsies (n = 6 per group) are significant for P values less than 0.05.

these targets did not differ between HF and LF muscles sampled at 110-kg body weight, as revealed by RT-PCR (data not shown).

DISCUSSION

Taking together the differences in mRNA levels and in protein abundance, a total of 40 unique genes were currently revealed as differentially expressed between HF and LF pig groups with a 3.5-fold difference in i.m. fat content at the same slaughter weight and age. This modest number of targets was somewhat unexpected, considering the fact that the powerful tools of transcriptomic and proteomic analyses have been associated in pig *Longissimus* muscles (LM). However, this was likely due to biological features rather than to technological considerations. First, although the porcine array is the most sensitive microarray for swine genomic studies (*31*), human microarrays have been also largely successful for identifying differentially expressed genes in pigs (*32*). The muscle-specific microarray considered here was also previously able to reveal a large pattern of genes associated with various meat quality traits in cattle (*19*). Second, Wang and colleagues (*11*) using a cattle muscle/fat cDNA have identified 24 individual genes as differentially expressed in a comparison study involving two cattle breeds with a different ability to deposit i.m. fat. In addition, Lee et al. (*33*) by using differential display RT-PCR, revealed only 14 genes in relation to i.m. fat development within the *Longissimus* muscle of cattle compared at two fattening time points.

To cope with technical limits inherent to the detection of low-abundance proteins by 2-DE, the proteomic procedure was performed for cytosolic extracts. Indeed, many pathways relevant to lipid fields occur in this fraction (e.g., glycolysis, lipolysis, lipogenesis, esterification, etc). On the contrary, almost the whole transcriptome of the same muscles was analyzed, including genes encoding proteins with cytoskeletal, trans-membrane and mitochondrial origins, and unique pathways for the regulation of transcription and chromatin assembly. This accounted for the lack of correlation (except *GSTP1*) between differentially regulated data generated by proteomic and transcriptomic methodologies. It seems also reasonable to speculate time-course differences between mRNA changes and protein responses. In support, we show the difference in ESD protein abundance in LM harvested in pigs at 110-kg body weight but changes in the ESD mRNA level only in muscle biopsies taken at 70-kg live weight.

This study reveals four main biological categories shared by transcriptomic and proteomic lists and prioritized proteins, peptides, and glucose metabolic processes as involved in differences between HF and LF pigs. A number of genes with a greater expression in HF pigs than in LF pigs are related to protein biosynthesis, including *MRPS21* encoding mitochondrial ribosomal proteins, *BARHL2* involved in transcriptional regulation, *DOLPP1* with a possible role in post-translational glycosylation, and protein DJ-1 engaged in folding of nascent polypeptides. Conversely, an over-representation of the major tool for extra-lysosomal protein degradation, i.e., the intact proteasome 26S and the subunit α type 1 of its catalytic core particle 20S, was demonstrated at the protein level in HF versus LF pig muscles; this was accompanied by up-regulation of the transcript of *RFN214* involved in protein tagging before degradation. All together, these results suggest the turnover of proteins to be involved in the i.m. fat content difference between HF and LF pigs. This is likely because proteins involved in the regulation of proliferation, differentiation, and cell cycling undergo not only biosynthesis but also degradation in a tightly regulated and temporally controlled fashion (*34*, *35*). In addition, HF pig muscles displayed a greater abundance in ENO1 and GAPDH glycolytic enzymes when compared to LF pig muscles. The glycolytic pathway is important in the first steps of glucose conversion into lipids, and de novo lipogenesis has been identified as an important pathway for i.m. fat content in pig muscles (*4*). Conversely, we show the lower abundance of ESD protein in muscles of HF pigs compared to that in LF pigs, and we confirm the same pattern for the *ESD* transcript in muscle biopsies taken in the same pigs at 70 kg live weight. Various lipases and esterases including ESD with a high homology to triacylglycerol hydrolase have been identified in mouse adipose tissue by RT-PCR (*36*) and 2-DE combined with mass spectrometry (*37*). Taken together with the lower abundance in HF pigs compared to LF pigs of a regulatory subunit (RIα) of the cAMP-dependent PKA with a putative role in regulating lipolysis (*38*), it is then likely that the orientation of the balance between lipogenesis to lipolysis has participated in the variation of i.m. fat content in those pigs. This is in accordance with the metabolic data obtained in adipocytes isolated from pig muscle showing a ratio of lipogenesis to lipolysis rather than the regulation of one of this pathways to be involved in adipocyte hypertrophy during pig growth (*39*). Finally, a protein belonging to the π class of glutathione *S*-transferases (GSTP1) was found to be up-regulated both at mRNA and protein abundance levels in HF pigs compared with that in LF pigs. In Japanese Black cattle with a high propensity to deposit i.m. fat, *GSTP1* was also found overexpressed compared to that in Holstein animals with small amounts of i.m. fat (*11*). However, the difference in *GSTP1* encoding a protein involved in cellular detoxification is likely the consequence rather than the cause of variability in i.m. fat content. In support of this assumption, both PRDX6 processing antioxidant properties (*40*) and the redox-sensitive molecular chaperone DJ-1 protein (*41*) also had a greater abundance in HF versus LF pigs. It is then likely that the extensive contribution of lipids to the muscle architecture in HF pigs forms a cellular environment particularly sensitive to lipid peroxidation.

Cell communication represents the second largest functional category elicited in the current study. Especially, two genes belonging to the family of G-protein-coupled receptors (*GPR-18* and *CXCR3*) had opposite expression patterns in HF pigs and LF pigs. It has been shown that different receptor isoforms of the GPR family exert opposing effects on cell proliferation (*42*). They cooperate to activate extracellular signal-regulated kinases and the MAPK cascade, through the transaction of the epidermal growth factor receptor (*EGFR*) (*43*). We found *EGFR* having a greater mRNA expression level in HF pigs than in LF pigs. Whether *GPR-18* and *CXCR3* have mediated differences in i.m. fat accumulation, however, remains to be demonstrated. A number of genes encoding the proteins of skeletal muscle structure are also shown to be differentially expressed between HF and LF pigs, such as cofilin 2 (*CFL2*) promoting filament assembly, the intermediate filament protein keratin 17 (*KRT17*), and Ca2+-binding protein parvalbumin (*PVALB*). This is in agreement with other data in cattle (*11*, *33*) pointing out many proteins of the skeletal muscle structure in relation to i.m. fat development. Finally, it remains to be demonstrated whether the down-regulation of matrix metallopeptidases (*MMP*)*24* observed in HF pigs and up-regulation of *TIMP2* as a tissue inhibitor of MMPs in the same pigs could have played an important role in extracellular matrix remodelling and adipogenesis (*44*, *45*) inside HF and LF pig muscles.

In a previous experiment (*7*), a greater number of intramuscular adipocytes have been demonstrated in pigs selected for high i.m. fat content compared to that in pigs selected on low i.m. fat content. In the current study, we detected a greater amount of mRNA of *FABP4* in HF biopsies than in LF ones. Because *FABP4* is expressed exclusively in adipocytes (*26*), the relative level in *FABP4* mRNA is likely indicative of the amount of i.m. adipose tissue or of the number of i.m. adipocytes in HF biopsies. Importantly, the functional categories underlined in our study are also rather similar to those identified during in vitro adipogenesis of bovine cells (*46*). In addition, we show the differential expression of genes that might have played key roles in regulating adipogenesis in biopsy specimens of HF and LF pigs taken at 70-kg live weight. The down-regulation of *HMGA1* expression in HF versus LF biopsies is in accordance with a negative role in adipocytic cell growth (*47*). *HMGA1* polymorphisms have also been consistently associated with fat deposition traits across several pig populations (*48*). Conversely, repression of cyclin D1 expression has been shown either to promote (*49*) or to inhibit (*28*) adipocyte differentiation and phenotype. Because some genes selected by the microarray experiment have possible links with the MAPK pathway, we also checked the expression levels of two members of the MAPK family. A lower expression of *p38MAPK14* was observed in HF biopsies compared to that in LF biopsies. This is consistent with the fact that the inhibition of the *p38MAPK* pathway and knockout of the *p38MAPK* gene led to an increased adipogenesis in

cellular models (*50*). Conversely, the expression level of *ERK1* did not differ between HF and LF biopsies, extending other recent results showing no difference in the total and the phosphorylation of ERK1/2 between beef muscles extremes for i.m. content (*51*). Because *HMGA1* and *p38* genes generally act on adipogenesis via the regulation of C/EBPs or PPARγ transcriptional activity, it remains questionable why we were not able to show significant differences in expression levels of these master regulators of adipogenesis between HF pigs and LF pigs. Cattle breeds with extreme performances in terms of i.m. fat deposition exhibit differences in the expression of C/EBPs in adipose tissues only at some particular times of the fattening period and not later in growth (*52*). Early stages in the growth period are then likely to be studied for a better understanding of variability in i.m. lipid content, although i.m. adipose tissue is laid down mainly in mature animals. However, the exact time frame after the first postnatal month [(i.e., the moment when the first adipocytes are identified in pig muscles (*14*)] remains to be determined.

LITERATURE CITED

(1) Wood, J. D.; Enser, M.; Fisher, A. V.; Nute, G. R.; Sheard, P. R.; Richardson, R. I.; Hughes, S. I.; Whittington, F. M. Fat deposition, fatty acid composition and meat quality: a review. *Meat Sci*. **2008**, *78*, 343–358.

(2) Fernandez, X.; Monin, G.; Talmant, A.; Mourot, J.; Lebret, B. Influence of intramuscular fat content on the quality of pig meat. 2. Consumer acceptability of muscle longissimus lumborum. *Meat Sci*. **1999**, *53*, 67–72.

(3) Poulos, S.; Hausman, G. Intramuscular adipocytes-potential to prevent lipotoxicity in skeletal muscle. *Adipocytes* **2005**, *1*, 79–94.

(4) Mourot, J.; Kouba, M. Development of intra- and intermuscular adipose tissue in growing Large White and Meishan pigs. *Reprod. Nutr. Dev*. **1999**, *39*, 125–132.

(5) Chen, J.; Yang, X. J.; Xia, D.; Chen, J.; Wegner, J.; Jiang, Z.; Zhao, R. Q. Sterol regulatory element binding transcription factor 1 expression and genetic polymorphism significantly affect intramuscular fat deposition in the longissimus muscle of Erhualian and Sutai pigs. *J. Anim. Sci*. **2008**, *86*, 57–63.

(6) Gerbens, F.; Jansen, A.; van Erp, A. J.; Harders, F.; Meuwissen, T. H.; Rettenberger, G.; Veerkamp, J. H.; te Pas, M. F. The adipocyte fatty acid-binding protein locus: characterization and association with intramuscular fat content in pigs. *Mamm. Genome* **1998**, *9*, 1022–1026.

(7) Damon, M.; Louveau, I.; Lefaucheur, L.; Lebret, B.; Vincent, A.; Leroy, P.; Sanchez, M. P.; Herpin, P.; Gondret, F. Number of intramuscular adipocytes and fatty acid binding protein-4 content are significant indicators of intramuscular fat level in crossbred Large White × Duroc pigs. *J. Anim. Sci*. **2006**, *84*, 1083–1092.

(8) Jurie, C.; Cassar-Malek, I.; Bonnet, M.; Leroux, C.; Bauchart, D.; Boulesteix, P.; Pethick, D. W.; Hocquette, J. F. Adipocyte fatty acid-binding protein and mitochondrial enzyme activities in muscles as relevant indicators of marbling in cattle. *J. Anim. Sci*. **2007**, *85*, 2660–2669.

(9) Essen-Gustavsson, B.; Karlsson, A.; Lundstrom, K.; Enfalt, A. C. Intramuscular fat and muscle fiber lipid contents in halothane-gene-free pigs fed high or low protein diets and its relation to meat quality. *Meat Sci*. **1994**, *38*, 269–277.

(10) Gondret, F.; Mourot, J.; Bonneau, M. Comparison of intramuscular adipose tissue cellularity in muscles differing in their lipid content and fibre type composition during rabbit growth. *Livest. Prod. Sci*. **1998**, *54*, 1–10.

(11) Wang, Y. H.; Byrne, K. A.; Reverter, A.; Harper, G. S.; Taniguchi, M.; McWilliam, S. M.; Mannen, H.; Oyama, K.; Lehnert, S. A. Transcriptional profiling of skeletal muscle tissue from two breedsof cattle. *Mamm. Genome* **2005**, *16*, 201–210.

(12) Wang, Y. H.; Reverter, A.; Mannen, H.; Taniguchi, M.; Harper, G. S.; Oyama, K.; Byrne, K. A.; Oka, A.; Tsuji, S.; Lehnert, S. A. Transcriptional profiling of muscle tissue in growing Japanese Black cattle to identify genes involved with the development of intramuscular fat. *Aust. J. Exp. Agri*. **2005**, *45*, 809–820.

(13) Kolditz, C. I.; Paboeuf, G.; Borthaire, M.; Esquerré, D.; SanCristobal, M.; Lefèvre, F.; Médale, F. Changes induced by dietary energy intake and divergent selection for muscle fat content in rainbow trout (*Oncorhynchus mykiss*), assessed by transcriptome and proteome analysis of the liver. *BMC Genomics* **2008**, *9*, 506.

(14) Hauser, N.; Mourot, J.; De Clercq, L.; Genart, C.; Remacle, C. The cellularity of developing adipose tissues in Pietrain and Meishan pigs. *Reprod. Nutr. Dev*. **1997**, *37*, 617–625.

(15) Daumas, G.; Dhorne, T. Teneur en viande maigre des carcasses de porc, évaluation et estimation. *Journées Rech. Porcine* **1997**, *29*, 411–418.

(16) Folch, J.; Lee, M.; Sloane Stanley, G. H. A simple method for the isolation and purification of total lipids from animal tissues. *J. Biol. Chem*. **1957**, *226*, 497–509.

(17) Monin, G.; Sellier, P. Pork of low technological quality with a normal rate of muscle pH fall in the immediate postmortem period: the case of the Hampshire breed. *Meat Sci*. **1985**, *13*, 49–63.

(18) Chomczynski, P.; Sacchi, N. Single-step method of RNA isolation by acid guanidium thiocyanate-phenol-chloroform extraction. *Anal. Biochem*. **1987**, *162*, 156–159.

(19) Bernard, C.; Cassar-Malek, I.; Le Cunff, M.; Dubroeucq, H.; Renand, G.; Hocquette, J. F. New indicators of beef sensory quality revealed by expression of specific genes. *J. Agric. Food Chem*. **2007**, *55*, 5229–5237.

(20) Blum, H.; Beier, H.; Gross, H. J. Improved silver staining of plant proteins, RNA and DNA in polyacrylamide gels. *Electrophoresis* **1987**, *8*, 93–99.

(21) Shevchenko, A.; Wilm, M.; Vorm, O.; Mann, M. Mass spectrometric sequencing of proteins from silver stained polyacrylamide gels. *Anal. Chem*. **1996**, *68*, 850–858.

(22) Le Meur, N.; Lamirault, G.; Bihouée, A.; Steenman, M.; Bédrine-Ferran, H.; Teusan, R.; Ramstein, G.; Léger, J. J.2004. A dynamic, web-accessible resource to process raw microarray scan data into consolidated gene expression values: importance of replication. *Nucleic Acids Res*. 2004, *8*, 5349-5358.

(23) Benjamini, Y.; Hochberg, Y. Controlling the false discovery rate, a practical and powerful approach to multiple testing. *J. Royal Statist. Soc., Ser. B* **1995**, *57*, 289–300.

(24) Zivy, M. Quantitative analysis of 2D gels. *Methods Mol. Biol*. **2007**, *355*, 175–94.

(25) Rolland, A. D.; Evrard, B.; Guitton, N.; Lavigne, R.; Calvel, P.; Couvet, M.; Jégou, B.; Pineau, C. Two-dimensional fluorescence difference gel electrophoresis analysis of spermatogenesis in the rat. *J. Proteome Res*. **2007**, *6*, 683–697.

(26) Chmurzyńska, A. The multigene family of fatty acid-binding proteins (FABPs): function, structure and polymorphism. *J. Appl. Genet*. **2006**, *47*, 39–48.

(27) Fajas, L.; Fruchart, J. C.; Auwerx, J. Transcriptional control of adipogenesis. *Curr. Opin. Cell Biol*. **1998**, *10*, 165–173.

(28) Hishida, T.; Naito, K.; Osada, S.; Nishizuka, M.; Imagawa, M. Crucial roles of D-type cyclins in the early stage of adipocyte differentiation. *Biochem. Biophys. Res. Commun*. **2008**, *370*, 289–294.

(29) Bost, F.; Aouadi, M.; Caron, L.; Binétruy, B. The role of MAPKs in adipocyte differentiation and obesity. *Biochimie* **2005**, *87*, 51–56.

(30) Pfaffl, M. W. A new mathematical model for relative quantification in real-time RT-PCR. *Nucleic Acids Res*. **2001**, *29*, e45.

(31) Tsai, S.; Mir, B.; Martin, A. C.; Estrada, J. L.; Bischoff, S. R.; Hsieh, W. P.; Cassady, J. P.; Freking, B. A.; Nonneman, D. J.; Rohrer, G. A.; Piedrahita, J. A. Detection of transcriptional

difference of porcine imprinted genes using different microarray platforms. *BMC Genomics* **2006**, *7*, 32.
(32) Moody, D. E.; Zou, Z.; McIntyre, L. Cross-species hybridisation of pig RNA to human nylon microarrays. *BMC Genomics* **2002**, *3*, 27.
(33) Lee, S. H.; Park, E. W.; Cho, Y. M.; Kim, S. K.; Lee, J. H.; Jeon, J. T.; Lee, C. S.; Im, S. K.; Oh, S. J.; Thompson, J. M.; Yoon, D. Identification of differentially expressed genes related to intramuscular fat development in the early and late fattening stages of Hanwoo steers. *J. Biochem. Mol. Biol*. **2007**, *40*, 757–764.
(34) Genini, D.; Catapano, C. V. Control of peroxisome proliferator-activated receptor fate by the ubiquitin-proteasome system. *J. Recept. Signal Transduct. Res* **2006**, *26*, 679–692.
(35) Zuo, Y.; Qiang, L.; Farmer, S. R. Activation of CCAAT/enhancer-binding protein (C/EBP) alpha expression by C/EBP beta during adipogenesis requires a peroxisome proliferator-activated receptor-gamma-associated repression of HDAC1 at the c/EBPalpha gene promoter. *J. Biol. Chem*. **2006**, *281*, 7960–7967.
(36) Shen, W. J.; Patel, S.; Yu, Z.; Jue, D.; Kraemer, F. B. Effects of rosiglitazone and high fat diet on lipase/esterase expression in adipose tissue. *Biochem. Biophys. Acta*. **2007**, *1771*, 177–184.
(37) Birner-Gruenberger, R.; Susani-Etzerodt, H.; Waldhuber, M.; Riesenhuber, G.; Schmidinger, H.; Rechberger, G.; Kollroser, M.; Strauss, J. G.; Lass, A.; Zimmermann, R.; Haemmerle, G.; Zechner, R.; Hermetter, A. The lipolytic proteome of mouse adipose tissue. *Mol. Cell Proteomics* **2005**, *4*, 1710–1717.
(38) Holm, C. Molecular mechanisms regulating hormone-sensitive lipase and lipolysis. *Biochem. Soc. Trans*. **2003**, *31*, 1120–1124.
(39) Gardan, D.; Gondret, F.; Louveau, I. Lipid metabolism and secretory function of porcine intramuscular adipocytes compared with subcutaneous and perirenal adipocytes. *Am. J. Physiol. Endocrinol. Metab*. **2006**, *291*, E372–380.
(40) Kang, S. W.; Baines, I. C.; Rhee, S. G. Characterization of a mammalian peroxiredoxin that contains one conserved cysteine. *Biol. Chem*. **1998**, *273*, 6303–6311.
(41) Shendelman, S.; Jonason, A.; Martinat, C.; Leete, T.; Abeliovich, A. DJ-1 is a redox-dependent molecular chaperone that inhibits alpha-synuclein aggregate formation. *PLoS Biol*. **2004**, *2*, e362.
(42) Sellers, L. A.; Alderton, F.; Carruthers, A. M.; Schindler, M.; Humphrey, P. P. A. Receptor isoforms mediate opposing proliferative effects through G$\beta\gamma$-activated p38 or AKt pathways. *Mol. Cell. Biol*. **2000**, *20*, 5974–5985.
(43) Daub, H.; Weiss, F. U.; Wallasch, C.; Ullrich, A. Role of transactivation of the EGF receptor in signaling by G-protein-coupled receptors. *Nature* **1996**, *379*, 557–560.
(44) Maquoi, E.; Munaut, C.; Colige, A.; Collen, D.; Lijnen, H. R. Modulation of adipose tissue expression of murine matrix metalloproteinases and their tissue inhibitors with obesity. *Diabetes* **2002**, *51*, 1093–1101.
(45) Christiaens, V.; Lijnen, H. R. Role of the fibrinolytic and matrix metalloproteinase systems in development of adipose tissue. *Arch. Physiol. Biochem*. **2006**, *112*, 254–259.
(46) Tan, S. H.; Reverter, A.; Wang, Y. H.; Byrne, K. A.; McWilliam, S. M.; Lehnert, S. A. Gene expression profiling of bovine in vitro adipogenesis using a cDNA microarray. *Funct. Integr. Genomics* **2006**, *6*, 235–249.
(47) Fedele, M.; Battista, S.; Manfioletti, G.; Croce, C. M.; Giancotti, V.; Fusco, A. Role of the high mobility groups A proteins in human lipomas. *Carcinogenesis* **2001**, *22* 1583–1591.
(48) Kim, K. S.; Thomsen, H.; Bastiaanse, J.; Nguyen, N. T.; Dekkers, J. C.; Plastow, G. S.; Rothschild, M. F. Investigation of obesity candidate genes on porcine fat deposition quantitative trait loci regions. *Obesity Res*. **2004**, *12*1981–1994.
(49) Wang, C.; Pattabiraman, N.; Zhou, J. N.; Fu, M.; Sakamaki, T.; Albanese, C.; Li, Z.; Wu, K.; Hulit, J.; Neumeister, P.; Novikoff, P. M.; Brownlee, M.; Scherer, P. E.; Jones, J. G.; Whitney, K. D.; Donehower, L. A.; Harris, E. L.; Rohan, T.; Johns, D. C.; Pestell, R. G. Cyclin D1 repression of peroxisome proliferator-activated receptor gamma expression and transactivation. *Mol. Cell. Biol*. **2003**, *23*6159–6173.
(50) Aouadi, M.; Laurent, K.; Prot, M.; Le Marchand-Brustel, Y.; Binétruy, B.; Bost, F. Inhibition of p38MAPK increases adipogenesis from embryonic to adult stages. *Diabetes* **2006**, *55*, 281–289.
(51) Underwood, K. R.; Means, W. J.; Zhu, M. J.; Ford, S. P.; Hess, B. W.; Du, M. AMP-activated protein kinase is negatively associated with intramuscular fat content in longissimus dorsi muscle of beef cattle. *Meat Sci*. **2008**, *79*, 394–402.
(52) Yamada, T.; Kawakami, S. I.; Nakanishi, N. Expression of adipogenic transcription factors in adipose tissue of fattening Wagyu and Holstein steers. *Meat Sci*. **2009**, *81*, 86–92.

Received for Review October 23, 2008. Accepted February 25, 2009. Revised manuscript received February 6, 2009. Jingshun Liu was supported by a grant from INRA (Animal Physiology and Livestock Systems Division).